

EFFECT OF HEAT TREATMENT AND IRRADIATION TEMPERATURE ON IMPACT BEHAVIOR OF IRRADIATED REDUCED-ACTIVATION FERRITIC STEELS—R. L. Klueh and D. J. Alexander (Oak Ridge National Laboratory)

Objective

The goal of this study is to evaluate the impact behavior of irradiated ferritic steels and relate the changes in properties to the heat treatment of the steel.

SUMMARY

Charpy tests were conducted on eight normalized-and-tempered reduced-activation ferritic steels irradiated in two different normalized conditions. Irradiation was conducted in the Fast Flux Test Facility at 393°C to ≈ 14 dpa on steels with 2.25, 5, 9, and 12% Cr (0.1% C) with varying amounts of W, V, and Ta. The different normalization treatments involved changing the cooling rate after austenitization. The faster cooling rate produced 100% bainite in the 2.25 Cr steels, compared to duplex structures of bainite and polygonal ferrite for the slower cooling rate. For both cooling rates, martensite formed in the 5 and 9% Cr steels, and martensite with $\approx 25\%$ δ -ferrite formed in the 12% Cr steel. Irradiation caused an increase in the ductile-brittle transition temperature (DBTT) and a decrease in the upper-shelf energy. The difference in microstructure in the low-chromium steels due to the different heat treatments had little effect on properties. For the high-chromium martensitic steels, only the 5Cr steel was affected by heat treatment. When the results at 393°C were compared with previous results at 365°C, all but a 5Cr and a 9Cr steel showed the expected decrease in the shift in DBTT with increasing temperature.

PROGRESS AND STATUS

Introduction

Reduced-activation or fast induced-radioactivity decay (FIRD) steels for fusion power plant applications are being developed at the Oak Ridge National Laboratory (ORNL) [1]. Eight experimental steels have been studied [2-4]. Nominal compositions of the eight ORNL steels are given in Table 1, along with the designation for each.

TABLE 1—Nominal compositions for reduced-activation steels

Alloy	Nominal Chemical Composition ^a (wt %)				
	Cr	W	V	Ta	C
2.25CrV	2.25		0.25		0.1
2.25Cr-1WV	2.25	1.0	0.25		0.1
2.25Cr-2W	2.25	2.0			0.1
2.25Cr-2WV	2.25	2.0	0.25		0.1
5Cr-2WV	5.0	2.0	0.25		0.1
9Cr-2WV	9.0	2.0	0.25		0.1
9Cr-2WVTa	9.0	2.0	0.25	0.12	0.1
12Cr-2WV	12.0	2.0	0.25		0.1

^a Balance iron.

Information on microstructure [2], tempering and tensile properties [3], and Charpy impact properties [4] of the eight FIRD steels in the normalized-and-tempered condition has been reported. Results were also published on the tensile properties after irradiation to 6-8 and 25-29 dpa and on the Charpy properties after irradiation at 365°C to 6-8, 15-17, 23-24, and 26-29 dpa in the Fast Flux Test Facility (FFTF) [5]. The results showed that the two 9Cr steels, especially the 9Cr-2WVTa,

compared to the other steels. The 2¼Cr-2WV steel was the strongest of the eight steels [3], but it had relatively poor impact properties, as was true for the impact properties of all of the low-chromium (2¼Cr) steels [4].

For ferritic steels, the heat treatment, which determines the microstructure, includes the cooling rate, which is determined by the cooling medium (i.e., air cool, water quench, etc.) and section size. This paper reports on the effect of irradiation on the Charpy properties of the eight ORNL steels after two different heat treatments: one treatment was the same as that used for previous irradiations [5]; in the other the steels were cooled more rapidly during normalization to produce 100% bainite in the 2¼Cr steels. Observations on Charpy properties after irradiation are useful because neutron irradiation causes an increase in the ductile-brittle transition temperature (DBTT) and a decrease in upper-shelf energy (USE). Such changes generally reflect a degradation in fracture toughness. Developing steels with minimal changes in DBTT and USE is crucial if ferritic steels are to be useful structural materials for fusion.

Experimental Procedure

Details on the processing and chemical composition of the eight steels have been published [2]. The steels were normalized and tempered prior to irradiation. The 2¼Cr-2W steel without vanadium was austenitized at 900°C. The other seven heats contained vanadium and were austenitized at 1050°C; the higher normalizing temperature assured that any vanadium carbide dissolved during austenitization. To determine heat treatment (microstructural) effects, especially for the low-chromium steels, two different geometries were normalized. First, 15.9-mm-thick plates were austenitized 1 h and then air cooled. This is the same heat treatment (termed HT1) used in the previous studies [2-6]. In the second heat treatment (HT2), 3.3-mm-square bars (the miniature Charpy specimens) were austenitized 0.5 h in a tube furnace in a helium atmosphere and then pulled into the cold zone of the furnace and cooled in flowing helium. For both HT1 and HT2, the 2¼CrV, 2¼Cr-1WV, and 2¼Cr-2W steel specimens were tempered 1 h at 700°C and the other five heats 1 h at 750°C.

One-third size Charpy specimens were machined from normalized-and-tempered 15.9-mm plates, along the rolling direction with the notch transverse to the rolling direction (L-T orientation). Details on the test procedure for the subsized Charpy specimens have been published [7].

Six Charpy specimens of each heat and each heat treated condition were irradiated in the Materials Open Test Assembly of FFTF at ~393°C. Specimens were irradiated to $\approx 2.3 \times 10^{26}$ n/m² (E>0.1 MeV), which produced ≈ 14 dpa. Helium concentrations were calculated to be less than 1 appm.

Results

Microstructures

Microstructures of the normalized-and-tempered 15.9-mm plates (HT1) were examined [2]. Of the low-chromium steels, all but the 2¼Cr-2W contained a duplex structure of tempered bainite and polygonal ferrite: 2¼CrV contained $\approx 30\%$ tempered bainite, 70% ferrite; 2¼Cr-1WV contained $\approx 55\%$ tempered bainite, 45% ferrite; and 2¼Cr-2WV was $\approx 80\%$ tempered bainite, 20% ferrite. The 2¼Cr-2W steel was 100% tempered bainite. When the 3.3-mm bars were heat treated, the microstructures for all four 2¼Cr steels were 100% bainite.

Microstructures were the same for the high-chromium steels when heat treated in either geometry: the 5Cr-2WV, 9Cr-2WV, and 9Cr-2WVt steels were 100% tempered martensite, and the 12Cr-2WV steel was tempered martensite with $\approx 25\%$ δ -ferrite.

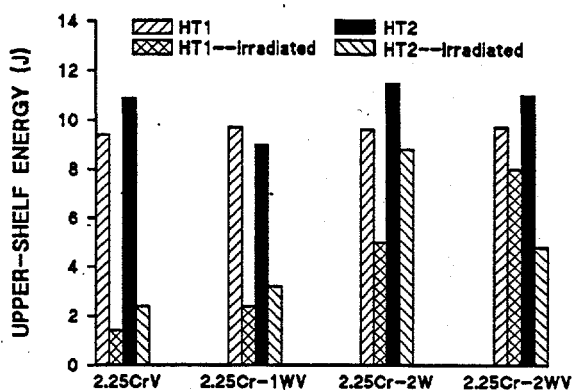
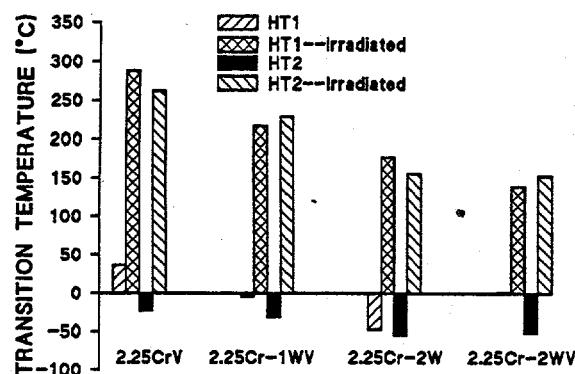


Fig. 1. Transition temperature and upper-shelf energy for low-chromium steels given two different heat treatments (HT1 and HT2) before and after irradiation.

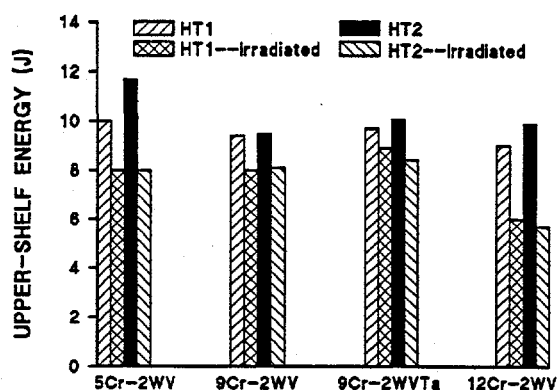
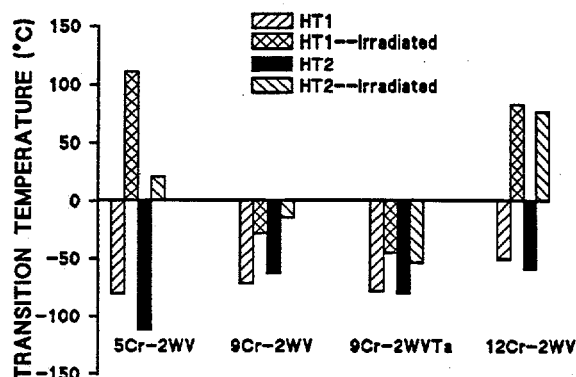


Fig. 2. Transition temperature and upper-shelf energy for high-chromium steels given two different heat treatments (HT1 and HT2) before and after irradiation.

Heat treatment to produce a 100% bainite microstructure (HT2) improved the DBTT of the 2¼Cr steels over those with the duplex structure (HT1) (Table 2 and Fig. 1). However, after irradiation, there was little difference in the DBTT of specimens given the HT1 and HT2 heat treatments and, in some cases, the shift in DBTT (Δ DBTT) was higher after HT2—especially for the 2¼Cr-2WV steel. Likewise, there was no significant difference in the USE after irradiation of the 2¼Cr steels with HT2 than for those with HT1.

Results for the high-chromium steels were somewhat more varied (Table 2 and Fig. 2). For the 5Cr-2WV steel, HT2 caused a significant improvement in the DBTT over that for HT1 (from -70 to -112), which translated into an improved Δ DBTT for the steel given HT2. Heat treatment had relatively little effect on the DBTT of the two 9Cr steels, either before or after irradiation. The DBTT of the 12Cr-2WV steel specimens given HT1 and HT2 heat treatments were quite similar before irradiation and had similar Δ DBTTs after irradiation. Heat treatment also had little effect on the USE of the high-chromium martensitic steels.

Table 2. Charpy impact properties of reduced-activation steels

Steel	Heat	DBTT	Δ DBTT	USE	Δ USE
2 $\frac{1}{2}$ CrV	HT1	36		9.4	
	HT1—Irrd	287	251	1.4	-85
	HT2	-24		10.9	
	HT2—Irrd	261	285	2.4	-78
2 $\frac{1}{2}$ Cr-1WV	HT1	-5		9.7	
	HT1—Irrd	216	221	2.4	-75
	HT2	-32		9.0	
	HT2—Irrd	228	260	3.2	-64
2 $\frac{1}{2}$ Cr-2W	HT1	-48		9.6	
	HT1—Irrd	176	224	5.0	-48
	HT2	-56		11.5	
	HT2—Irrd	155	211	8.8	-23
2 $\frac{1}{2}$ Cr-2WV	HT1	0		9.7	
	HT1—Irrd	138	138	8.0	-18
	HT2	-52		11.0	
	HT2—Irrd	152	204	4.8	-56
5Cr-2WV	HT1	-80		10.0	
	HT1—Irrd	111	191	8.0	-20
	HT2	-112		11.7	
	HT2—Irrd	21	133	8.0	-32
9Cr-2WV	HT1	-71		9.4	
	HT1—Irrd	-28	43	8.0	-15
	HT2	-63		9.5	
	HT2—Irrd	-14	49	8.1	-15
9Cr-2WV/Ta	HT1	-78		9.7	
	HT1—Irrd	-45	33	8.9	-8
	HT2	-80		10.1	
	HT2—Irrd	-53	27	8.4	-17
12Cr-2WV	HT1	-50		9.0	
	HT1—Irrd	83	133	6.0	-33
	HT2	-59		9.9	
	HT2—Irrd	77	136	5.7	-42

*HT1: normalized and tempered as 15.9-mm plate. HT2: normalized and tempered as 3-mm bar. Irrd: irradiated to \approx 15 dpa.

Discussion

This irradiation experiment had two objectives: 1) determine whether the microstructure of the 2¼Cr steels could be changed by heat treatment to favorably affect the Charpy impact properties after irradiation and 2) irradiate the reduced-activation steels in FFTF at a temperature other than 365°C, the temperature of previous irradiations [6]. The different heat treatments were not expected to cause significant changes in the microstructures of the 5-12% Cr steels, since the high hardenability of these steels would be expected to give them the same microstructure for both heat treatments. Specimens irradiated at 393°C in this experiment were expected to have a smaller Δ DBTT than those irradiated at 365°C [6], since the shift is due to irradiation hardening and irradiation hardening decreases with increasing irradiation temperature.

The relatively high DBTT values for the 2¼CrV, 2¼Cr-1WV, and 2¼Cr-2WV steels from the 15.9-mm plate (HT1) before irradiation were tentatively attributed to the ferrite in the mixed ferrite-bainite structures [5]. Only the 2¼Cr-2W steel had a low DBTT, and it was 100% tempered bainite [5]. Subsequent work indicated that heat treatment affected the unirradiated properties of three of the 2¼Cr steels (see Table 2) [7]. The DBTT of the 3.3-mm bar of 2¼Cr-2W steel was relatively unchanged: -48°C when heat treated as 15.9-mm plate (HT1) and -56°C when heat treated as 3.3-mm bar (HT2). For the other three 2¼Cr steels, the specimens given HT2 had considerably lower DBTT values than those given HT1. Thus, it appeared that the conclusion that high DBTT values were caused by the ferrite in the mixed ferrite-bainite microstructure of the unirradiated steels was correct [7].

As expected, there was little difference in the DBTT for HT1 and HT2 for the 9Cr-2WV, 9Cr-2WV/Ta, and 12Cr-2WV steels (Table 2). Microstructures were unchanged from 100% martensite for the 9Cr steels and 20-25% δ -ferrite, balance martensite for the 12Cr-2WV steel, regardless of the size of specimen heat treated. Although the microstructure of the 5Cr-2WV steel was 100% martensite and the DBTT of this steel was not expected to change, it showed a decrease for HT2 compared to HT1. The reason for this is unclear.

The previous results for the normalized-and-tempered 2¼Cr steels indicated that if it were possible to either use thinner sections, quench instead of normalizing, or improve the hardenability of the steels, it may be possible to lower the DBTT to make these steels attractive for fusion reactor applications [7]. The results of the present experiment indicate that it is somewhat more complicated than that when the steels are irradiated. Despite the decrease in DBTT caused by HT2 compared the HT1, there was no advantage for HT2 after irradiation.

It was previously shown that the bainite that forms in the 2¼Cr steels is not the same in all four steels [7]. Bainite, which is generally defined as a ferrite matrix containing carbides that forms in the temperature range 250-550°C, was originally thought to have only two morphological variations—upper and lower bainite [9]. Classical upper and lower bainite can be differentiated by the appearance of the carbide particles relative to the axis of the bainitic ferrite plate or needle. Upper bainite forms as a collection of ferrite plates or laths with carbides forming on the boundaries between the plates or laths. Lower bainite consists of ferrite plates or needles with carbides forming within the ferrite plates or needles at about a 60° angle to the axis of the plate or needle [9].

There are important variations on the classical bainites, as first shown by Habraken [10]. He found morphological variants in the bainite transformation products that differed from upper and lower bainite, although these products formed in the bainite transformation temperature regime. These "nonclassical" bainites formed more easily during a continuous cool than during isothermal transformation [10,11], where classical bainites are generally formed.

Habraken and Economopoulos contrasted the morphology of the nonclassical structures formed during continuous cooling with classical bainites obtained during isothermal transformation [11].

Classical upper and lower bainites form when the steel is transformed in different temperature regimes of the bainite transformation temperature region, as defined on an isothermal-transformation (IT) diagram [11]. This means that the bainite transformation region of an IT diagram can be divided into two temperature regimes by a horizontal line, above which upper bainite forms and below which lower bainite forms. For the nonclassical bainites, Habraken and Economopoulos [11] showed that a continuous cooling transformation (CCT) diagram could be divided into three vertical regions. Three different nonclassical bainite microstructures form when cooling rates are such as to pass through these different zones. Two of those microstructures are of interest here.

A steel cooled rapidly enough to pass through the first zone produces a "carbide-free acicular" structure, which consists of side-by-side plates or laths [11]. When cooled somewhat more slowly through the second zone, a carbide-free "massive or granular" structure results, generally referred to as granular bainite [11]. Granular bainite consists of a ferrite matrix with a high dislocation density that contains martensite-austenite (M-A) "islands" [11].

Microstructures in the 15.9-mm plates of the 2¼Cr-2W and 2¼Cr-2WV consisted of carbide-free acicular bainite and granular bainite, respectively [7]. During tempering, large globular carbides form in the M-A islands of the granular bainite, whereas elongated carbides form on lath boundaries of acicular bainite [7]. When the 3-mm bars were normalized, carbide-free acicular bainite also formed in the 2¼Cr-2WV steel [7]. Although no TEM was performed on the 2¼CrV and 2¼Cr-1WV, a similar microstructure is expected for these steels.

The results for the 2¼Cr steels in the present experiment indicate that neither the carbide-free acicular structure obtained by heat treating the 3-mm bars nor the granular bainite previously irradiated provides a microstructure that is resistant to irradiation. The large globular carbides that form in granular bainite can provide crack nucleation sites in the normalized-and-tempered condition, and these carbides grow during irradiation. Likewise, it appears that the interlath carbides in the acicular bainite can also be quite large and provide crack nucleation sites.

Because the 2¼Cr-2WV steel was the strongest of the eight steels in the unirradiated condition and because it is possible to produce a high density of small precipitates in a low-chromium steel that cannot be produced in the high-chromium steel (considering concentrations similar to those in Table 1), it has been suggested that the low-chromium steels may offer some advantages for fusion [3,7]. Results from the present experiment appear to contradict that suggestion—certainly for the compositions and heat treatments used here.

The acicular structures of the 2¼Cr steels irradiated in the present work contained fairly large intra- and inter-lath M_3C and M_7C_3 carbides formed during tempering [3,7]. These carbides can provide crack nucleation sites for fracture, just as the large globular carbides produced during tempering of the granular bainite can. The solution to a more irradiation-resistant steel might be to cool still more rapidly to minimize carbon segregation during cooling that lead to the large carbides when tempered. Alternatively, a vanadium-containing steel should be produced that develops a fine vanadium-rich MC precipitate without the large amounts of M_3C and M_7C_3 that formed in the 2¼Cr steels used here. The latter might be accomplished by using a lower tempering temperature on the acicular bainite or by developing a steel that does not need to be tempered. An alternative to the rapid cooling is to increase the hardenability. This can be done by changing the chemical composition, and a 3Cr-3WV steel has been developed that shows a significant improvement in the Charpy impact properties in the unirradiated condition [12]. This superiority was present even when tempered at 700°C or in the untempered condition. However, the irradiation resistance of this steel still needs to be determined.

Because of the high hardenability of the high-chromium (5-9% Cr) steels, no effect of cooling rate on Charpy properties was expected, and none was observed for the 9Cr and 12Cr steels (Fig. 2).

An effect was observed, however, for the 5Cr-2WV steel (a DBTT of -80°C for the 15.9-mm plate and -112°C for the 3.3-mm bar). All indications were that there was no major difference in the microstructures of the unirradiated plate and bar for the high-chromium steels. Even the grain sizes were similar, although the plate was austenitized 1 h at 1050°C , while the smaller bar was austenitized 0.5 h at 1050°C .

The major difference in the microstructure of the high-chromium steels in the unirradiated condition is the precipitates. The primary precipitate in the 9Cr and 12Cr steels is M_{23}C_6 ; in the 5Cr steel, it is M_7C_3 [3]. Both steels contain vanadium-rich MC, and the 5Cr steel contains a small amount of M_{23}C_6 . It may be that some M_7C_3 can precipitate in the 5Cr-2WV steel during the slow cool (in the 15.9-mm plate), which could affect the subsequent precipitate morphology during tempering. This is strictly speculation, since no transmission electron microscopy (TEM) has been performed on the steels heat treated as 3.3-mm bar in the normalized-and-tempered condition, and there has been no TEM on the 5Cr-2WV after irradiation. The only change observed for the 9Cr steels after irradiation to 36 dpa at 420°C was the formation of dislocation loops estimated to be 40-100 nm in diameter at a number density of $3 \times 10^{15}/\text{cm}^3$ [13].

When the DBTT values obtained previously after irradiation to ≈ 16 dpa at 365°C are compared to those observed after ≈ 14 dpa at 393°C in the present experiment, the DBTTs of the 2 $\frac{1}{2}$ Cr chromium steels (Fig. 3) and the 12Cr-2WV steel (Fig. 4) were higher (larger ΔDBTT) after irradiation at 365°C than after the irradiation at 393°C . This is expected, since the shift in DBTT

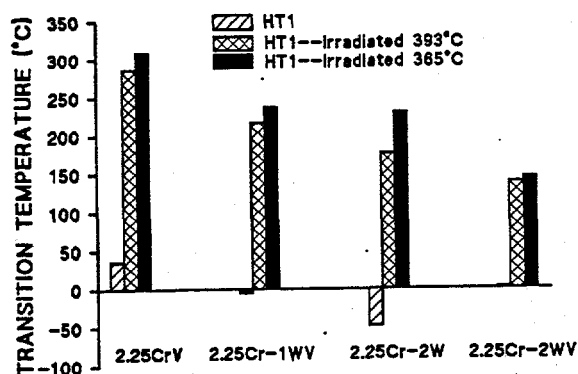


Fig. 5. Transition temperature of the low-chromium steels in HT1 and after irradiation to ≈ 15 dpa at 365°C and ≈ 14 dpa at 393°C .

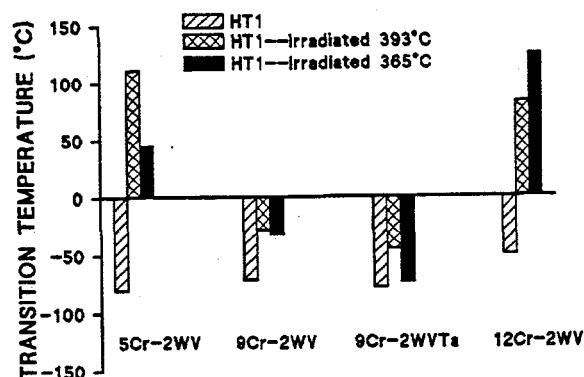


Fig. 6. Transition temperature of the high-chromium steels in HT1 and after irradiation to ≈ 15 dpa at 365°C and ≈ 14 dpa at 393°C .

is directly related to irradiation hardening, and irradiation hardening decreases with increasing irradiation temperature. Just the opposite behavior occurred for the 5Cr-2WV and the 9Cr-2WVTa (Fig. 4) with DBTT values of 45°C (16.7 dpa) and 111°C (15 dpa) at 365 and 393°C , respectively, for the 5Cr-2WV steel and -74°C (15.4 dpa) and -45°C (15 dpa), respectively, for the 9Cr-2WVTa steel. The 9Cr-2WV steel had DBTT values of -32°C (16.7 dpa) at 365°C and -28°C (15 dpa) at 393°C —a slight increase with increasing temperature (Fig. 4). However, after irradiation at 365°C to 7.7, 23.9, and 27.6 dpa, this steel had DBTT values of 8, -8, and 1°C , respectively, making it appear that the saturation value is higher, around 0°C , and the value at 16.7 dpa is in error. Therefore, it was concluded that the DBTT of the 9Cr-2WV steel at 365°C probably saturates a value somewhat higher than that found after irradiation at 393°C .

As pointed out above, the 5Cr-2WV steel shows a much larger ΔDBTT for HT1 than for HT2 when irradiated at 393°C ; it is HT1 that is being compared at the different temperatures. For the two 9Cr

steels, there was little difference for HT1 and HT2, and the difference between the 5Cr-2WV and 9Cr-2WV steels, which only differ in chromium concentration, may be related to the difference in primary precipitates in the 5Cr and 9Cr steel (M_7C_3 in the 5Cr and $M_{23}C_6$ in the 9Cr). The observation of an inverse temperature effect (a larger $\Delta DBTT$ at 393°C than 365°C) strengthens the conclusion that precipitates may play a role in the 5Cr-2WV steel. One role of carbide particles during fracture is to act as nucleation sites for the cracks that cause the failure [14,15]. As the size of a brittle precipitate particle increases, so too the size of the initial crack at fracture initiation can increase. Thus a possible reason why the 5Cr steel had a higher DBTT after irradiation at 393°C than at 365°C is that precipitates can grow to a larger size by irradiation-enhanced diffusion at the higher irradiation temperature. It is the larger precipitates that then cause the inverse effect with temperature for this steel. TEM is required to verify this suggestion.

The unexpected results for the 5Cr-2WV steel on the effect of heat treatment and irradiation temperature suggest that the DBTT after irradiation can be improved by decreasing the size of the precipitates. Precipitate size could be decreased by lowering the tempering temperature, and previous work indicated that the 5Cr-2WV steel has excellent Charpy properties even after tempering 1 h at 700°C, as opposed to the 750°C used in the present experiment [5].

The 9Cr-2WVTa steel has the best Charpy properties after irradiation of any of the steels tested here, and in other irradiation experiments it has been shown to have the lowest $\Delta DBTT$ for this type of steel ever observed [6,16, 17]. However, it also showed the inverse temperature effect. After 15 dpa at 365°C, the $\Delta DBTT$ for HT1 was only 14°C compared to 27°C after 14 dpa at 393°C (Table 2). An inverse temperature effect was noted previously when the steel was irradiated to 0.8 dpa at 250-450°C in the High Flux Reactor (HFR) in Petten, the Netherlands [16]. Figure 5 shows the properties of the 9Cr-2WVTa steel (labeled ORNL) irradiated along with several other reduced-activation steels (F82H, OPTIFER I and OPTIFER II) and conventional Cr-Mo steels (MANET I and II) in the HFR at 250-450°C to 0.8 dpa. The ORNL 9Cr-2WVTa steel had the lowest DBTT below $\approx 375^\circ\text{C}$ [16]. This superior behavior has now been verified for irradiation to 2.5 dpa in HFR [17]. The inverse temperature effect was displayed by the 9Cr-2WVTa steel in that the DBTT increases above 400°C (Fig. 5), in the temperature regime where hardening is expected to decrease to low values, which should translate to low values of DBTT. Indeed, no such increase was observed for the other steels.

The origin of the superior behavior for the 9Cr-2WVTa has been sought by comparing the behavior of this steel, the 9Cr-2WV steel, which is the same as the 9Cr-2WVTa but without tantalum, and the conventional 9Cr-1MoVNb steel [6]. The 9Cr-2WV and 9Cr-2WVTa steels were irradiated at 365°C in FFTF, with the 9Cr-2WVTa steel showing exceptionally small $\Delta DBTT$ s: 4, 14, 21, and 32°C after 6.4, 15.4, 22.5, and 27.6 dpa, respectively (the value after 15.4 dpa is plotted in Fig. 4) [6]. The $\Delta DBTT$ for the 9Cr-2WV saturated at $\approx 60^\circ\text{C}$, which was reached by ≈ 8 dpa (the lowest irradiation fluence). This compares with the 9Cr-1MoVNb and irradiated to ≈ 4 dpa at 365°C in FFTF, which saturated at $\approx 45^\circ\text{C}$ [6].

When the 9Cr-2WV, 9Cr-2WVTa, and 9Cr-1MoVNb steels with HT1 were compared, it was found that the difference in Charpy properties of these steels before and after irradiation occurred despite there being little difference in the strength of the 9Cr-2WVTa and the other two steels before and after irradiation [6]. Transmission electron microscopy examination of the normalized-and-tempered 9Cr-2WV and 9Cr-2WVTa revealed only minor differences prior to irradiation [3,13]. Likewise, there was no marked difference in microstructure after irradiation, with similar numbers of dislocation loops formed in both steels [13]. Thus, the similarity in strength of these two steels before and after irradiation is not unexpected. However, without any gross differences in the microstructure of the two steels, the only other major difference to account for the difference in Charpy properties is the tantalum in solid solution. Based on the amount of tantalum that appeared to be present in the carbides of the 9Cr-2WVTa steel prior to irradiation, it was estimated that most of the tantalum remained in solid solution [13]. An atom probe analysis of the unirradiated steel

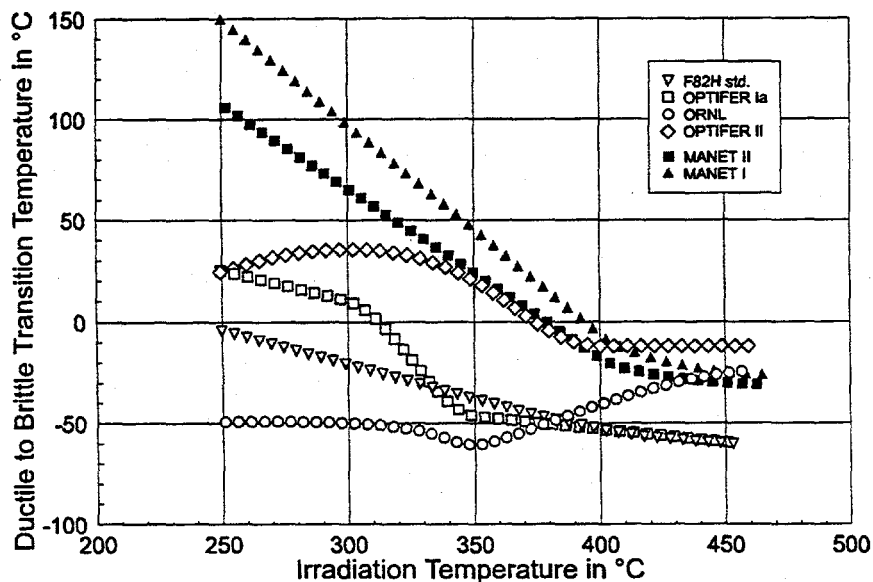


Fig. 5. Transition temperature as a function of temperature for four reduced-activation and two conventional martensitic steels irradiated to 0.8 dpa in the HFR. Taken from Rieth et al. [16].

9Cr-2WVTa steel indicated that >90% of the tantalum was in solution in the normalized-and-tempered condition [18].

Tantalum in solution in the 9Cr-2WVTa can probably account for the smaller prior-austenite grain size in that steel than in the 9Cr-2WV [6]. A smaller lath (subgrain) size might also be expected but was not observed in two studies [3,13], although a smaller lath size was observed in a third examination [18]. The smaller prior-austenite grain size was originally used to explain the difference between the 9Cr-2WV and 9Cr-2WVTa steels [19], since a smaller grain size can lead to a lower DBTT in the normalized-and-tempered condition. However, this explanation was subsequently questioned, because in the normalized-and-tempered condition, the two steels had similar yield stresses, and they also had a yield stress similar to that of the 9Cr-1MoVNb, which had the smallest grain size of the three steels [6]. After saturation, the Δ DBTT of the 9Cr-2WV and 9Cr-1MoVNb were similar, but above the value for the 9Cr-2WVTa [6]. This occurred despite there being only minor differences in the microstructural changes that occurred in the 9Cr-2WVTa and 9Cr-1MoVNb during irradiation, while the microstructural changes in the 9Cr-2WV and 9Cr-2WVTa were similar [13].

These observations led to the conclusion that microstructure (grain size, precipitate type, etc.) does not provide the sole explanation for the observations on mechanical property changes. It appears that tantalum in solution must cause a higher fracture stress for 9Cr-2WVTa than 9Cr-2WV, and the combination of tungsten and tantalum in the 9Cr-2WVTa leads to a higher fracture stress than produced by the combination of molybdenum and niobium in 9Cr-1MoVNb steel [6].

There has been work to determine how alloying elements affect the DBTT, for example, why nickel and platinum decrease the transition temperature of iron alloys and silicon increases it [20,21]. The DBTT can be changed by either decreasing the flow stress or increasing the fracture stress. Since there is little difference in the strength of the steel with and without tantalum, it has been suggested that tantalum increases the fracture stress [19].

To understand the fracture process, Griffith [22,23] considered the balance between the energy released by elastic relaxation and that required for the creation of new surface area during growth of a crack in a brittle material; for a through crack, he found that

$$\sigma_f = \left(\frac{2E\gamma_s}{\pi a(1-\nu^2)} \right)^{1/2}, \quad (1)$$

where σ_f is the stress at fracture, E is Young's modulus, γ_s is the true surface energy, ν is Poisson's ratio, and a is the crack half-length. Orowan [24] and Irwin [25] suggested that the true surface energy should be replaced by an effective surface energy, γ_e , which would include the plastic work done during fracture. For an embedded penny-shaped crack, as would result from initiation at a carbide particle or at an inclusion, or from a crack forming within an entire grain or other microstructural unit, this equation becomes [26]

$$\sigma_f = \left(\frac{4E\gamma_p}{D(1-\nu^2)} \right)^{1/2}, \quad (2)$$

where D is the crack diameter. An additional factor can be included to account for elliptically shaped particles [27].

For a ferritic steel with spherical carbide particles, the diameter of the carbide particle can be used for the crack diameter, D . This could not be used to account for the observations on 9Cr-2WVTa, however, since there appears to be no difference in the amount or morphology of the precipitates in the 9Cr-2WV and 9Cr-2WVTa [3,13].

In the case of a bainitic or martensitic steel, the packet or lath size can be used as the crack size. As stated above, one study found a difference in the lath size of the normalized-and-tempered 9Cr-2WV and 9Cr-2WVTa steels [18], two other studies found no difference [3,13]. More importantly, no difference was observed after irradiation to 36 dpa at 420°C in FFTF [13]. Therefore, lath size does not appear to offer an explanation. If the increase in DBTT with dose and irradiation temperature observed in the 9Cr-2WVTa was due to increasing lath (sub-grain) size during irradiation, then a similar effect might be expected for other ferritic/martensitic steels, which is not the case. That is, other such steels would be expected to show subgrain growth, which would result in increasing DBTT with increasing fluence; instead, most steels show a saturation in the shift in DBTT with increasing fluence. Prior austenite grain size could also be considered as the crack size, but this does not explain the change in DBTT for the same reason lath size does not, as the prior austenite grain size does not change during irradiation.

After eliminating prior austenite grain size, lath size, and carbides, Eq. (2) indicates that the explanation must involve Young's modulus or the effective surface energy. The small amount of tantalum added will have little if any effect on the modulus. Gerberich et al. found effects of nickel and silicon on the effective surface energy for binary iron-based alloys [21], and concluded that a change in fracture stress could explain why nickel caused a decrease and silicon caused an increase in the transition temperature of binary Fe-Ni and Fe-Si alloys. As pointed out in the previous section, the shift in DBTT for 9Cr-2WVTa steel increases with irradiation dose and irradiation temperature. This may be due to the removal of tantalum from solution; this suggestion needs to be confirmed. The effects of microstructural parameters on the transition temperature are complex, as Gerberich et al. [21] have noted; the ductile-brittle transition model for iron and iron-binary alloys that they derived involved 19 flow and fracture parameters.

Thus, microstructural changes (grain size, precipitate type, etc.) cannot provide the sole explanation for the observations on mechanical property changes. It appears that tantalum in solution must change the effective surface energy, which causes a higher fracture stress for 9Cr-2WVTa than 9Cr-2WV, and the combination of tungsten and tantalum in the 9Cr-2WVTa leads to a higher fracture stress than produced by molybdenum and niobium in 9Cr-1MoVNb [6].

The observation that the Δ DBTT of the 9Cr-2WVTa appeared to increase slightly with fluence [6] would follow if tantalum is being removed from solution during irradiation and being incorporated in the existing or new precipitates. This can also explain the increase in DBTT for the 9Cr-2WVTa irradiated above 400°C (Fig. 5). The increase occurs at >400°C, where irradiation-enhanced diffusion, even after only 0.8 dpa, may permit a reduction of tantalum in solution. In the present experiment (Fig. 4), the better properties observed after irradiation to 15 dpa at 365°C than after 14 dpa at 393°C may be the result of more tantalum being removed from solution at the higher irradiation temperature. If this is the case, the Δ DBTT of the 9Cr-2WVTa would be expected to increase with fluence as tantalum is removed from solution, just as is observed at 365°C [6]. Eventually, it might be expected to approach the Δ DBTT for the 9Cr-2WV. Even if that were to happen, however, the 9Cr-2WVTa should still have the lowest DBTT after irradiation because of its lower DBTT before irradiation [6].

5. Summary and Conclusion

Charpy impact properties were determined on eight reduced-activation Cr-W ferritic steels irradiated in FFTF to \approx 14 dpa at 393°C. To determine the effect of heat treatment, specimens were taken from normalized-and-tempered 15.9-mm plate and 3.3-mm bar. Chromium concentrations in the steels ranged from 2.25 to 12 wt% (all steels contained 0.1%C). The 2¼Cr steels contained variations of tungsten and vanadium (2¼CrV, 2¼Cr-1WV, 2¼Cr-2W) and steels with 2.25, 5, 9, and 12% Cr contained a combination of 2% W and 0.25% V (2¼Cr-2WV, 5Cr-2WV, 9Cr-2WV, and 12Cr-2WV). A 9Cr steel containing 2% W, 0.25% V, and 0.07% Ta (9Cr-2WVTa) was also irradiated. The microstructure of the 2¼Cr steels in the 15.9-mm plate were bainite with various amounts of polygonal ferrite, and they were 100% bainite when heat treated as 3.3-mm bar. The 5Cr steel and the two 9Cr steels were 100% martensite and the 12Cr steel was martensite with \approx 25% δ -ferrite after heat treatment in either geometry.

The change in microstructure of the 2¼Cr steels from a duplex structures of bainite plus ferrite to 100% bainite caused by heat treatment resulted in improvement in the Charpy properties before irradiation. After irradiation, however, there was little difference in the properties for the two different heat treatments. As expected, cooling rate had little effect on the high-chromium (9 and 12% Cr) steels. The Charpy properties for the 5Cr-2WV steel were improved by the faster cooling rate of the 3.3-mm bar. The reason for this change is unclear, but it may be caused by the different precipitates present in the 5Cr steel as compared to the other martensitic steels (M_7C_3 is present in the 5Cr-2WV steel but not in the other martensitic steels).

Results from the present irradiation experiment were compared with previous experiments for irradiation at a lower temperature (365°C). The DBTT values of all but the 5Cr-2WV and 9Cr-2WVTa steels were lower after irradiation at 393°C than after irradiation at 365°C, which is the expected behavior. The contrary behavior of the 5Cr steel was tentatively attributed to the M_7C_3 carbides that form in this composition that are not present in the 9Cr and 12Cr steels. The inverse temperature effect in the 9Cr-2WVTa steel was suggested to be due to the loss of tantalum from solution during irradiation at the higher temperature. It was concluded that the tantalum in solution gives the 9Cr-2WVTa steel its advantage over the other steels, and this advantage is decreased by its loss during irradiation..

References

- [1] R. L. Klueh, K. Ehrlich, and F. Abe, *J. Nucl. Mater.* 191-194 (1992) 116.
- [2] R. W. Conn et al., Panel Report on Low Activation Materials for Fusion Applications, University of California, Los Angeles, PPG-753, March 1983.
- [3] R. L. Klueh and P. J. Maziasz, *Met. Trans.* 20A (1989) 373.
- [4] R. L. Klueh, *Met. Trans.* 20A (1989) 463.
- [5] R. L. Klueh and W. R. Corwin, *J. of Mater. Engr.* 11 (1989) 169.
- [6] R. L. Klueh and D. J. Alexander, in: *Effects of Radiation on Materials: 18th International Symposium, ASTM STP 1325*, Eds. R. K. Nanstad, M. L. Hamilton, F.A. Garner, and A.S. Kumar (American Society for Testing and Materials, Philadelphia, 1997) to be published.
- [7] R. L. Klueh, P. J. Maziasz, and D. J. Alexander, *J. Nucl. Mater.* 179-181 (1991) 679.
- [8] D. J. Alexander, R. K. Nanstad, W. R. Corwin, and J. T. Hutton, in: *Applications of Automation Technology to Fatigue and Fracture Testing, ASTM STP 1092*, Eds. A. A. Braun, N. E. Ashbaugh, and F. M. Smith (American Society for Testing and Materials, Philadelphia, 1990) p. 83.
- [9] R. W. K. Honeycombe, *Steels: Microstructures and Properties* (Edward Arnold Ltd, London, 1981), p.106.
- [10] L. J. Habraken, *Proc. 4th Int. Conf. Electron Microscopy, Vol. 1* (Springer-Verlag, Berlin, 1960) p. 621.
- [11] L. J. Habraken and M. Economopoulos, *Transformation and Hardenability in Steels* (Climax-Molybdenum Company, Ann Arbor, MI, 1967) p. 69.
- [12] R. L. Klueh, D. J. Alexander, and P. J. Maziasz, *Met. Trans.* 28A (1997) 335.
- [13] J. J. Kai and R. L. Klueh, *J. Nucl. Mater.* 230 (1996) 116.
- [14] R. W. Hertzberg, *Deformation and Fracture Mechanics of Engineering Materials*, 3rd Edition (John Wiley & Sons, New York, 1989) p. 253.
- [15] C. J. McMahon, Jr., *Fundamental Phenomena in the Materials Sciences, Vol. 4*, L. J. Bonis, J. J. Duga, and J. J. Gilman, Eds. (Plenum Press, New York, 1967) p. 247.
- [16] M. Rieth, B. Dafferner, and H. D. Röhrig, *J. Nucl. Mater.*, 233-237 (1996) 351.
- [17] K. Ehrlich, Private Communication, October 24, 1996.
- [18] R. Jayaram and R. L. Klueh, to be published.
- [19] R. L. Klueh and D. J. Alexander, *J. Nucl. Mater.*, 212-215 (1994) 736.
- [20] W. C. Leslie, *The Physical Metallurgy of Steels* (McGraw-Hill, New York, 1981) 122.
- [21] W. W. Gerberich, Y. T. Chen, D. G. Atteridge, and T. Johnson, *Acta Met.*, 29 (1981) 1187.
- [22] A. A. Griffith, *Phil. Trans. R. Soc. London*, 221A (1920) 163.
- [23] A. A. Griffith, *Proc. 1st Intl. Cong. Appl. Math.* (Delft, The Netherlands, 1924) 55.
- [24] E. Orowan, *Rep. Prog. Phys.* 12 (1948-1949) 185.
- [25] G. R. Irwin, in: *Fracture of Metals* (American Society for Metals, Cleveland, OH, 1948) 147.
- [26] R. A. Sack, *Proc. Phys. Soc. London*, 58 (1946) 729.
- [27] H. L. Ewalds and R. J. H. Wanhill, *Fracture Mechanics* (Edward Arnold Ltd., London, 1984) 43.